ORGANIC CHEMISTRY

A concise synthesis of tetrodotoxin

David B. Konrad[1]†‡, Klaus-Peter Rühmann[2]‡, Hiroyasu Ando[3], Belinda E. Hetzler[2], Nina Strassner[4], Kendall N. Houk[4], Bryan S. Matsuura[2]*‡, Dirk Trauner[2]*§

Tetrodotoxin (TTX) is a neurotoxic natural product that is an indispensable probe in neuroscience, a biosynthetic and ecological enigma, and a celebrated target of synthetic chemistry. Here, we present a stereoselective synthesis of TTX that proceeds in 22 steps from a glucose derivative. The central cyclohexane ring of TTX and its α-tertiary amine moiety were established by the intramolecular 1,3-dipolar cycloaddition of a nitrile oxide, followed by alkynyl addition to the resultant isoxazoline. A ruthenium-catalyzed hydroxylactonization set the stage for the formation of the dioxa-adamantane core. Installation of the guanidine, oxidation of a primary alcohol, and a late-stage epimerization gave a mixture of TTX and anhydro-TTX. This synthetic approach could give ready access to biologically active derivatives.

Tetrodotoxin (TTX) is a neurotoxic natural product that has inspired and empowered chemists and biologists for more than a century (*1*–*3*). As a selective blocker of voltage-gated sodium channels, it has played a crucial role in the elucidation of the action potential, and it is still routinely used to silence excitable cells in neural systems. Its isolation from widely differing species, such as pufferfish, starfish, sea snails, octopi, toads, and newts, has prompted intense investigations into its true biological producers, its biosynthesis, and its ecological role. It is now clear that TTX is synthesized by bacteria and accumulated by metazoan hosts as a defense against predators (*4*). Its toxicology and therapeutic utility in humans have been studied for decades and are still a topic of ongoing research (*5*).

As a synthetic target, TTX has been celebrated for the sheer intellectual challenge it provides and for the opportunity to demonstrate methodological and strategic advances. Its simple carbon framework, consisting of a cyclohexane ring with C1 and C2 side chains, stands in stark contrast to the dense network of polar functional groups that adorn it. Two hydroxy groups in a *syn* relationship engage a carboxylate as an ortho acid to form the signature dioxa-adamantane core of TTX, which is fused to a cyclic guanidine via an α-tertiary amine. One primary, two secondary, and a tertiary hydroxy group, as well as a hemiaminal, contribute further to the structural complexity of the molecule, which features four rings and nine contiguous stereocenters.

[1]Department of Chemistry, Ludwig-Maximilians-Universität München, Butenandtstr. 5-13, 81377 Munich, Germany. [2]Department of Chemistry, New York University, 100 Washington Square East, New York, NY 10003, USA. [3]Graduate School of Infection Control Sciences and Kitasato Institute for Life Sciences, Kitasato University, Tokyo, Japan. [4]Department of Chemistry and Biochemistry, University of California, Los Angeles, CA 90095, USA. ***Corresponding author. Email: b2matsuura@gmail.com (B.S.M.); dtrauner@upenn.edu (D.T.)**
†Present address: Department of Pharmacy, Ludwig-Maximilians-Universität München, Butenandtstr. 5-13, 81377 Munich, Germany.
‡These authors contributed equally to this work.
§Present address: Department of Chemistry, University of Pennsylvania, Philadelphia, PA 19104-6323, USA.

The first total synthesis of TTX, in racemic form, by Kishi and Fukuyama in 1972 stands as a landmark achievement in organic synthesis that, at the time, seemed hard to surpass (*6*). After a pause of more than 30 years, Isobe and co-workers published the first asymmetric synthesis in 2003 (*7*). This was followed shortly by the Hinman and Du Bois' asymmetric synthesis (2003) (*8*), a second Isobe approach (2004) (*9*, *10*), and a racemic and two asymmetric syntheses by Sato's group (2005, 2008 and 2010, respectively) (*11*–*13*). In 2017 and 2020, Fukuyama, Yokoshima, and colleagues revisited the molecule and published two distinct asymmetric routes to TTX (*14*, *15*). In addition, several studies have been published that intercept late-stage intermediates of the previous syntheses e.g., by the Alonso (2010) (*16*, *17*), Ciufolini (2015) (*18*–*20*), and Hudlicky (2018) (*21*) groups. Other approaches toward the molecule have been outlined (*3*, *22*, *23*).

An analysis of previous syntheses revealed several common features that motivated us to pursue a distinct strategy: (i) The cyclohexane core was either incorporated in the starting material, or was formed early, and then oxygens were added using epoxidations, dihydroxylations, or allylic oxidations of strategically placed alkenes. (ii) The α-tertiary amine on C8a was established via C–N bond formation, which must overcome considerable steric hindrance. Several methods have been implemented to address this challenge, such as intramolecular nitrogen transfer (sigmatropic rearrangement, aza-conjugate addition, nitrene insertion) and intermolecular S_N1-type nucleophilic substitution. (iii) The dioxa-adamantane was always formed spontaneously with careful orchestration of the sequence to adjust the oxidation state of C10 and set the labile C9 stereocenter. (iv) Every synthesis introduces the guanidine at a late stage (*7*, *24*) and uses protecting groups amenable to global deprotection in the final step.

Our synthetic analysis was guided by an attempt to link the formation of the cyclohexane core with the establishment of the α-tertiary amine as closely as possible, in contrast to previous total syntheses in which these strategic key steps were largely independent (*17*). To this end, we established a linear precursor that contained all the oxygen functionalities of the TTX skeleton, which would then be conjoined by a ring-forming reaction. This would be followed by installation of the α-tertiary amine through C–C bond formation, to introduce the C2 fragment that would eventually be incorporated into the dioxa-adamantane. Finally, we needed to develop a method to oxidize and lactonize this C2 fragment in a highly efficient manner.

Our ultimate retrosynthetic analysis is summarized in Fig. 1. Although not all compounds shown therein were defined in such detail at the outset of our study, it captures the essence of our synthetic plan. We reasoned that we could trace TTX back from an oxidation of an alkynyl isoxazolidine of type **1**, which would stem from bicyclic isoxazoline **2**, the product of an intramolecular 1,3-dipolar cycloaddition. Nitromethane would serve as a key linchpin in the assembly of **2**, reacting first in an intermolecular Henry reaction with aldehyde ***3***, followed by a dehydration to generate a reactive nitrile oxide intermediate that would close the central cyclohexane ring within a (3+2) cycloaddition. We have previously developed an asymmetric synthesis of unsaturated aldehydes similar to ***3*** via a Kiyooka aldol reaction and used it toward kweichowenol A, a polyoxygenated cyclohexene isolated from the plant *Uvaria kweichowensis* (*25*). Although an analogous route gave the aldehyde ***3*** in sufficient quantities to proceed with the synthesis of TTX, we found it more practical and economical to start from the glucose-derived building block **4**. All the carbons of glucose and two of its stereocenters would be retained over the course of the synthesis, making this an attractive starting material.

Previously known exo-methylene building block **5** was synthesized in three steps on a decagram scale from commercially available glucose derivative **4** and was also used by Sato and colleagues in their approach to TTX (see supplementary materials) (*13*). Regioselective reductive cleavage of the benzylidene acetal placed a benzyl ether at C5, yielding **6** (Fig. 2). A subsequent dihydroxylation then installed the tertiary alcohol with the correct absolute configuration at C6, as well as the C11 primary alcohol of TTX, providing **7** in excellent yield and as a single diastereomer (*26*). Protection of the vicinal diol as the acetonide, followed by an Appel reaction, gave the primary iodide **8**. Under conditions developed by Soengas and Silva, **8** underwent a reductive cleavage upon treatment with *tert*-butyl lithium at low temperature, to yield a δ,ε-unsaturated aldehyde (**12**, Fig. 3), which engaged in a Henry reaction in situ upon addition of nitromethane. This afforded nitro alcohols **9a**,**b** as a separable 1:1 mixture of diastereomers (*27*).

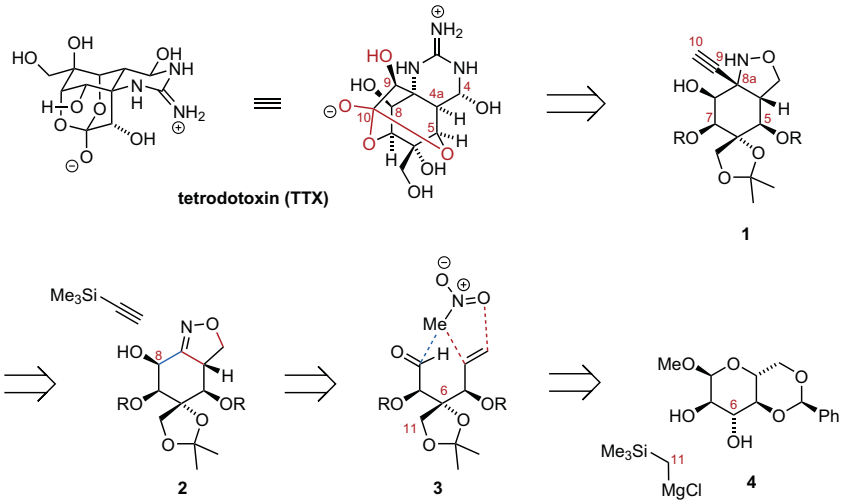

Fig. 1. Retrosynthetic analysis and synthetic design.

With nitro alcohols **9a**,**b** in hand, we were ready to attempt the key nitrile oxide cycloaddition to form the cyclohexane core of tetrodotoxin. Treatment of diastereomer **9a** with phenyl isocyanate and catalytic amounts of triethylamine triggered a dehydrative nitrile oxide cycloaddition, yielding isoxazoline **10** in moderate yield as a single diastereomer (*28*). An x-ray crystallographic structure of a byproduct, *N*-phenyl carbamate **11**, confirmed the configurations of the C8 and C4a stereocenters. Although the C4a stereocenter was inverted with respect to TTX, we reasoned that this isoxazoline diastereomer would be more accessible to nucleophiles for the formation of the hindered α-tertiary amine (*29*). Exposing diastereomer **9b** to the same reaction conditions only resulted in decomposition.

The poor diastereoselectivity of the Henry reaction and low yields of the cycloaddition severely hampered material throughput. Moving forward, we needed to develop a strategy that would selectively install the stereocenter at C8—ideally with a protected hydroxyl—which is critical in the ensuing cycloaddition. We reasoned that this could be accomplished via a dehydration to the corresponding nitroalkene followed by a conjugate addition with an appropriate *O*-nucleophile. This was realized by subjecting **8** to the same reductive fragmentation and Henry reaction sequence, followed by in situ dehydration, which yielded nitroalkene **14** exclusively as the *E*-isomer. **14** underwent an oxa-Michael addition upon treatment with the lithiated alkoxide of *p*-anisyl alcohol, presumably resulting in nitronate anion **15**. This intermediate could be intercepted with Boc-anhydride (via **16**) to trigger the formation of the transient nitrile oxide **17** and subsequent 1,3-dipolar cycloaddition, affording isoxazoline **18** in high yield and on a decagram scale (*30*). This reaction cascade was exquisitely diastereoselective, affording the central cyclohexane core of TTX with the correct configuration at C8, albeit with the wrong configuration at C4a.

Both the diastereoselectivity of the oxa-Michael addition and the mechanism of the 1,3-dipolar cycloaddition were further explored with quantum mechanical density functional theory calculations (see supplementary materials). The addition of PMB alkoxide, which resulted in the stereoselective formation of **15**, was shown to be favored by at least 3.4 kcal/mol (ΔG^{273K}) relative to the other five possible transition states. In the major transition state, the carbon chain adopts an *anti*-configuration with respect to the forming bond, as the Felkin-Anh model proposes, and the alkoxy group is *sym* to the double bond, an "inside alkoxy" arrangement shown to be favored for related cycloadditions (*31*).

The 1,3-dipolar cycloaddition can proceed through two possible pathways, initiated either by elimination of the *tert*-butyl carbonate (Boc-OH), followed by nitrile oxide cycloaddition, or by cycloaddition of the Boc-nitronate, followed by Boc-OH elimination. Calculations show that an elimination of Boc-OH proceeds quickly with a barrier of only 9.9 kcal/mol (ΔG^{298K}), whereas both cycloadditions occur with barriers of ~23 kcal/mol. Thus, the nitrile oxide pathway is strongly favored (see supplementary materials for details). The computational investigation further highlights a clear preference for the experimentally observed stereoisomer at C4a with a free energy difference of 1.4 kcal/mol. Although both transition states (shown in supplementary materials) adopt chair conformations, the one favoring the observed product avoids a 1,3-diaxial interaction of the alkoxy groups.

After deprotection of the *p*-methoxybenzyl (PMB) group with ceric ammonium nitrate (CAN), **10** was subjected to lithiated trimethylsilyl (TMS)–acetylide which, in the presence of $BF_3{\cdot}OEt_2$, underwent addition from the convex face of the bicyclic isoxazoline (*32*). After cleavage of the TMS group upon workup, isoxazolidine alkyne **19** was isolated as a single diastereomer, which possessed all the skeletal carbons of TTX and five out of its nine stereocenters with the correct absolute configuration. The presence of a free hydroxy group in **10**, which presumably coordinates to the nucleophile after deprotonation, was found to be crucial for the success of the addition to the oxime ether moiety. Isoxazoline **18**, by contrast, gave very low conversion. The lithiated TMS-acetylide was highly effective, whereas more functionalized C2 synthons were found to be unreactive.

Our next goal was the oxidative elaboration of the alkyne to introduce the stereogenic C9 alcohol and the C10 lactone that would ultimately engage in the formation of the signature ortho acid of TTX. Our original strategy was to form the requisite hydroxylactone via a gold- or silver-catalyzed 5-endo-dig hydroetherification of the C8 hydroxy group of **19** onto the alkyne terminus (Fig. 4A). Oxidation of the resultant dihydrofuran to a hydroxylactone, followed by isomerization, via a translactonization during the final deprotection, would unveil the central ortho acid. Unfortunately, extensive experimentation proved that this approach is exceptionally difficult to execute, requiring us to reexamine our sequence of bond-forming events. The logical solution to this conundrum would be to engage the alkyne terminus in a bridge-forming hydroetherification with either the C5 or C7 hydroxy group, followed by oxidation to the desired hydroxylactone, which would obviate the need for a translactonization step. However, this strategic shift was not without risk, as such bridge-forming 6-endo-dig cyclizations have scarce precedent.

To this end, we needed to establish a protecting group scheme that would also be compatible with the subsequent introduction of the guanidine moiety and the final steps. Exposure of **19** to Boc_2O gave **20**, which features both a *tert*-butyl carbonate and carbamate moiety. The next critical deprotection step required the simultaneous cleavage of the C5 and C7 benzyl ethers in the presence of the alkyne and isoxazolidine groups, which are sensitive to hydrogenation conditions, as well as three acid-sensitive protecting groups. After considerable experimentation, we found that the benzyl ethers could be cleanly removed by using Pieber and Seeberger's recently introduced chromoselective photochemical debenzylation (*33*), a singularly effective protocol that afforded diol **21** in excellent yield. The Boc-group on the C8-alcohol and the use of a 525-nm green light-emitting diode as the irradiation source were key to this reaction's success. The use of either the unprotected alcohol or higher-energy blue light resulted in complete substrate decomposition. Following the debenzylation, a selective methanolysis of the carbonate gave a triol, which could be protected to bis-acetonide **22**. At this stage, we elected to

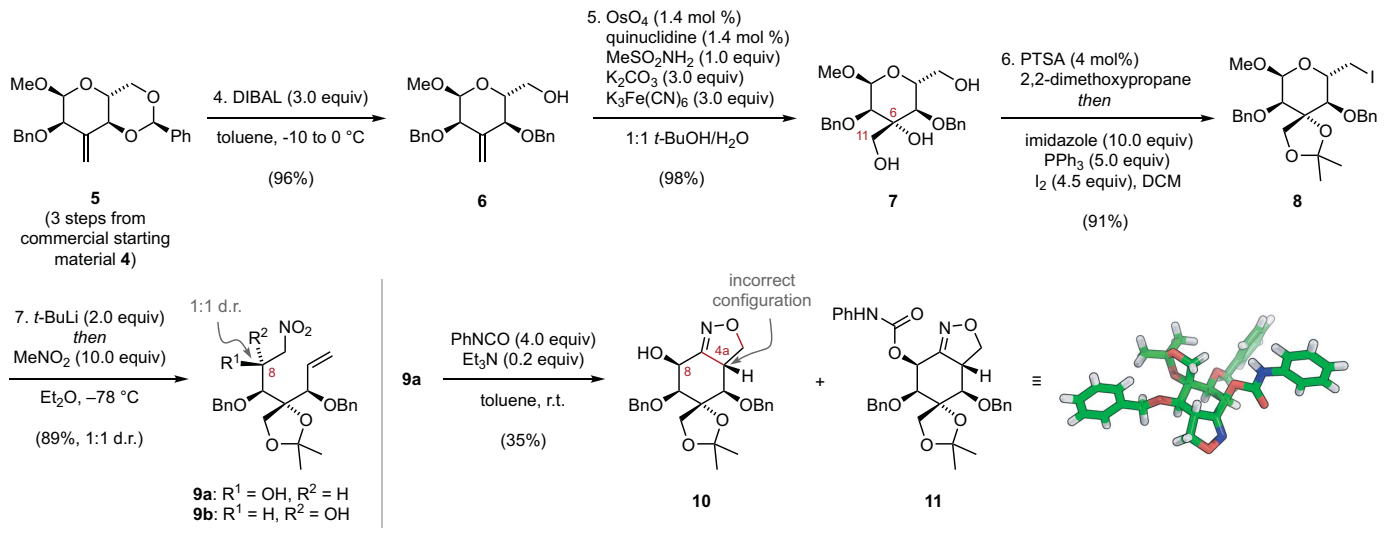

Fig. 2. Opening sequence and initial attempts to form the carbocyclic core. DIBAL, diisobutylaluminium hydride; PTSA, *p*-toluene sulfonic acid; DCM, dichloromethane; PhNCO, phenylisocyanate; r.t., room temperature.

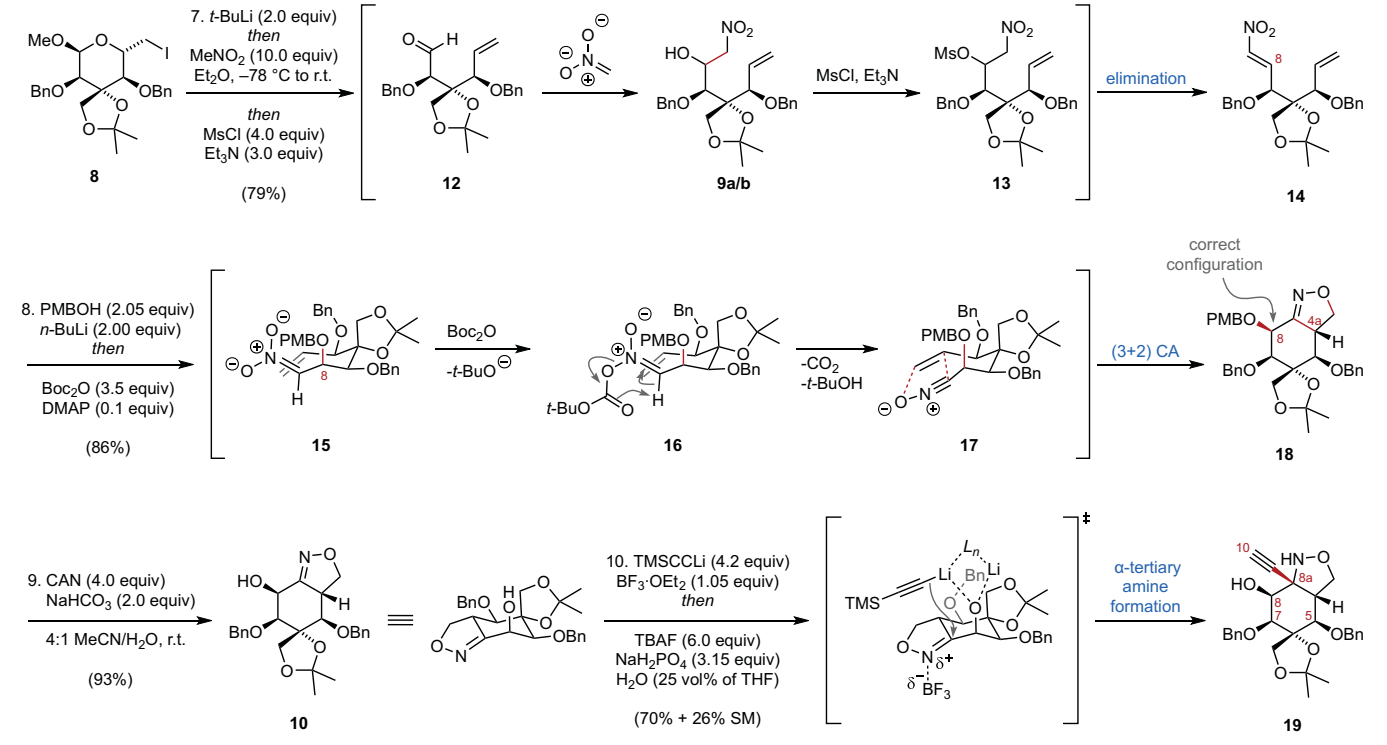

Fig. 3. Development of a diastereoselective route to the cyclohexane core and installation of the α-tertiary amine. MsCl, methanesulfonyl chloride; PMBOH, *p*-methoxybenzyl alcohol; Boc_2O, di-*tert*-butyl dicarbonate; DMAP, 4-dimethylaminopyridine; (3+2) CA, (3+2) cycloaddition; CAN, ceric ammonium nitrate; TMSCCLi, lithium trimethylsilylacetylide; TBAF, tetra-*n*-butylammonium fluoride; THF: tetrahydrofuran.

reduce the sensitive *N*-Boc isoxazolidine. By using SmI_2, the N–O bond was cleaved in excellent yield, resulting in a primary alcohol, which was then protected as its silyl ether **23** (Fig. 4A).

The stage was now set for the next key step of our synthesis, the conversion of alkyne **23** to hydroxylactone **25**. To take full advantage of the steric environment provided by the proximal acetonide, we aimed at forming the C10-O5 bond first to yield a dihydropyran that could then be oxidized to the hydroxylactone in a stereoselective manner. Initially, we attempted to achieve this via a 6-endo-dig cyclization with gold- or silver-based π-acid catalysts, but this approach was thwarted by the substrate's propensity to undergo an undesired 5-exo-dig cyclization.

Our solution to this problem was inspired by reports from Trost (*34*) and McDonald (*35*) on the catalytic generation of metallo-vinylidene carbenes, which would render the alkyne terminus (C10) electrophilic. We found that **23** could be converted to bridged dihydropyran **24**, with $CpRu(PPh_3)_2Cl$ as a cycloisomerization catalyst, in nearly quantitative yield on a 300-mg scale (*36*). Pushing this finding even further, we postulated that the resultant dihydropyran could be converted to the key hydroxylactone **25** by transforming the cycloisomerization catalyst into an oxidant. This hypothesis was supported by Blechert and co-workers, who demonstrated that ring-closing metathesis could be coupled with olefin dihydroxylation on simple bis-alkenes by using Ru-based metathesis catalysts (*37*). However, we would need to identify conditions that would further oxidize the hypothetical diol to the hydroxylactone, without overoxidation of

the desired product (e.g., oxidative cleavage or ketolactone formation). This was achieved by the addition of Oxone and a cosolvent mixture to the reaction (*38*). Presumably, under these conditions, the catalyst is oxidized to RuO_4, which, in turn, oxidized **24** to the desired hydroxylactone **25** with almost complete diastereoselectivity (Fig. 4B). We believe the chemoselectivity of the second oxidation is due to the increased hydricity of the C10–H bond of the hemiacetal intermediate. This single reaction combines the C10-O5 bond formation with two oxidation events, setting the C9 stereocenter in the processes, and had the added benefit of simplifying the purification, because the cycloisomerization catalyst was copolar with **24** on silica (*39*).

Having found a satisfying solution for the hydroxylactone problem, we decided to install

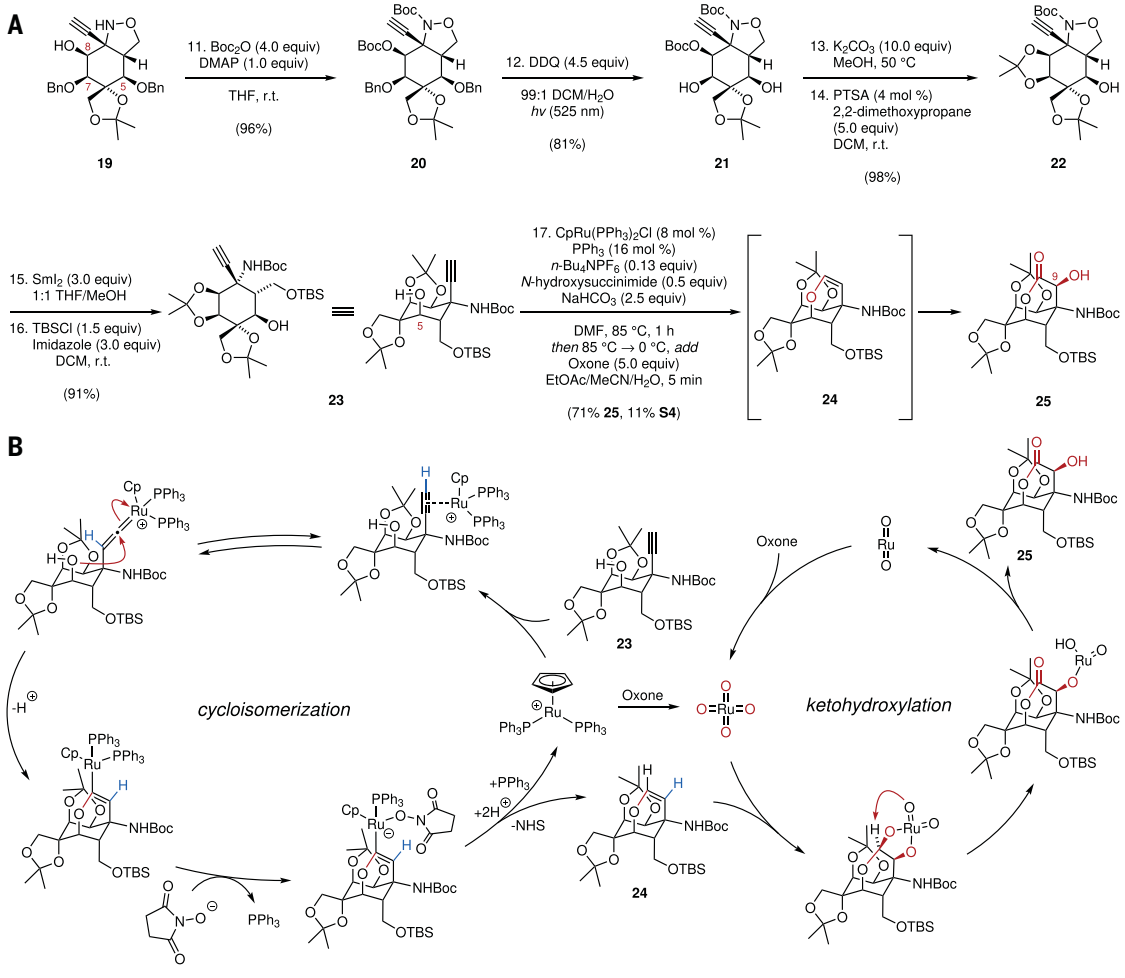

Fig. 4. Continuation of the synthesis and proposed mechanism for the key hydroxylactonization. (**A**) Synthesis. (**B**) Proposed mechanism. DDQ, 2,3-dichloro-5,6-dicyano-1,4-benzoquinone; TBSCl, *tert*-butyldimethylsilyl chloride; DMF, dimethylformamide; Cp, cyclopentadienyl.

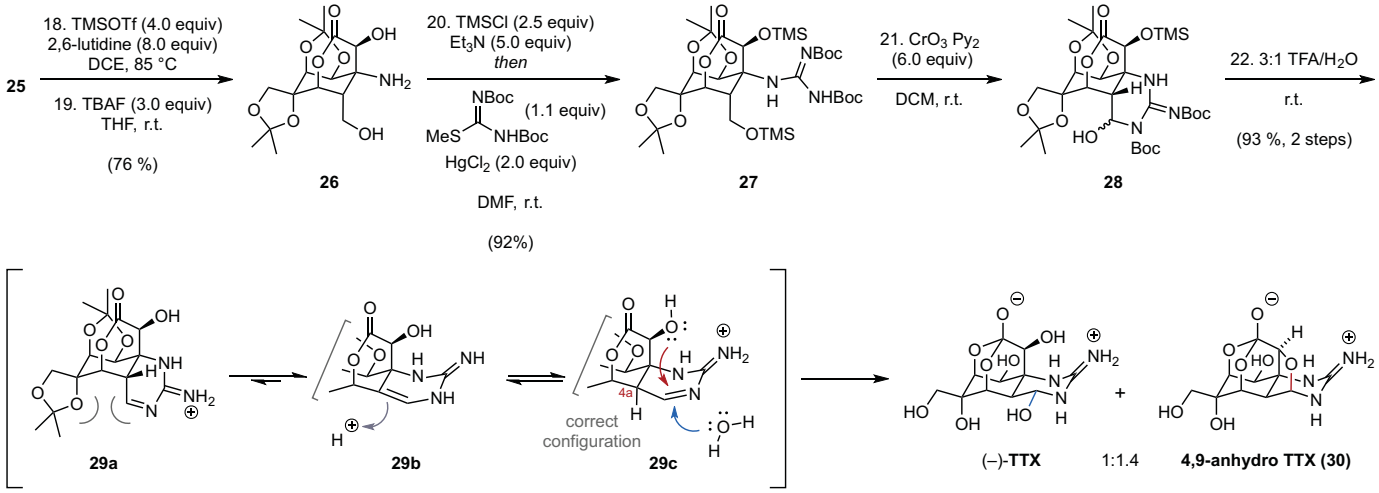

Fig. 5. Completion of the synthesis. TMSOTf, trimethylsilyl triflate; DCE, 1,2-dichloroethane; Py, pyridine; TFA, trifluoroacetic acid.

the guanidine moiety next. Removal of the *N*-Boc protecting group with trimethylsilyl triflate, followed by cleavage of the silyl ethers, one of which was transient, gave amino diol **26**. This compound was protected in situ as the bis-trimethyl silyl ether and then underwent clean guanylation under Kishi's conditions to afford compound **27**, which features all the atoms of TTX (Fig. 5).

In the last phase of our synthesis, we had to overcome two final obstacles: the oxidation of the primary silyl ether and the epimerization of the C4a stereocenter. A footnote in Kishi's seminal publication suggested the latter presented a potential liability owing to the propensity of the C5-O bond to undergo facile elimination, and all prior approaches had set this stereocenter earlier in their respective syntheses (*6*). Nevertheless, we continued by treating bis-trimethyl silyl ether **27** with Collins reagent, which effected selective deprotection and oxidation of the primary alcohol, resulting in **28** as a mixture of hemiaminal isomers. This transformation could not have been performed with a more stable *tert*-butyl dimethyl silyl ether in place, that is, with a guanidinylated derivative of compound **25**. Crude **28** was then dissolved in 25% aqueous trifluoroacetic acid and stirred at room temperature overnight. Notably, this effected the desired deprotections, epimerization, and cyclizations and gave a 1:1.4 mixture of TTX and 4,9-anhydro TTX (**30**) in good yield. We observed the formation of **30** in unusually high proportions, which could be explained by the guanidine participating in the epimerization process. Intramolecular condensation of the N3 nitrogen with the C4a aldehyde would form a highly stabilized iminium cation **29a**, which could undergo elimination to enamine **29b**. Protonation to the more thermodynamically favored iminium **29c** situates the electrophilic C4 in close proximity to the C9 hydroxy group, which can attack at a rate that is kinetically competitive with solvolysis. We believe that the elimination and tautomerization reactions are likely driven by unfavorable *syn*-pentane interactions between the C6 oxygen and the C4 iminium. However, given the multitude of transformations that are taking place in this final step, it is difficult, if not impossible, to pinpoint the exact sequence of events, which could take place in parallel and converge on TTX. TTX and **30** are known to be in equilibrium with one another, favoring TTX, and they can be readily interconverted (*7*, *40*). Indeed, upon heating of this mixture for 3 days as a solution in 5% d_3-AcOD–95% D_2O to 60°C, a 2.9:1 ratio of TTX and anhydro-TTX (**30**) was obtained (see supplementary materials). TTX and **30** have been separated on an analytical scale (*41*).

Taking stock of our strategic disconnections, our route showcases the power of the Huisgen cycloaddition for the construction of highly substituted cyclitols. For this purpose, the humble C1 synthon nitromethane performed spectacularly—involved in no fewer than six bond-forming and -breaking events—relaying an oxygen to C4, and embedding its nitrogen and carbon into the α-tertiary amine over the course of the synthesis. Although the bicyclic isoxazoline **10** possessed the incorrect stereocenter at C4a, necessitating a late-stage epimerization, it guided the subsequent acetylide addition from the convex face of the molecule to install the desired configuration of the C8a α-tertiary amine. Although this late-stage epimerization carried some strategic risk, we had reason to believe that it would succeed based on the coherence of the dioxa-adamantane core, which would render β-eliminations or retro-aldol reactions reversible. The alkynylation of **10** emphasizes the utility of oxime ethers as α-tertiary amine precursors but also highlights the need for more methodological development in this area. The Ru-catalyzed oxidative lactonization of alkyne **23** represents a notable advance in establishing the C9 and C10 hydroxylactone and should have future applications in the synthesis of other natural products such as the ginkolides and quassinoids (*42*, *43*). Furthermore, this synthesis served as a proving ground for the chromoselective photochemical debenzylation and recognizes the strategic value of implementing new technology and methods in highly complex settings.

Taken together, these strategic decisions resulted in one of the shortest and the most efficient syntheses of tetrodotoxin to date, accomplishing this goal in 22 total steps and 11% overall yield from commercially available starting materials. Our route is scalable and can be adapted to the production of other scarce tetrodotoxin derivatives to better understand their biosynthesis and chemical ecology. It is also amenable for the procurement of TTX derivatives that could serve as next-generation analgesics.

REFERENCES AND NOTES

1. J. Chau, M. A. Ciufolini, *Mar. Drugs* **9**, 2046–2074 (2011).
2. T. Nishikawa, M. Isobe, *Chem. Rec.* **13**, 286–302 (2013).
3. M. Makarova, L. Rycek, J. Hajicek, D. Baidilov, T. Hudlicky, *Angew. Chem. Int. Ed.* **58**, 18338–18387 (2019).
4. C. T. Hanifin, *Mar. Drugs* **8**, 577–593 (2010).
5. E. G. Moczydlowski, *Toxicon* **63**, 165–183 (2013).
6. Y. Kishi *et al*., *J. Am. Chem. Soc.* **94**, 9219–9221 (1972).
7. N. Ohyabu, T. Nishikawa, M. Isobe, *J. Am. Chem. Soc.* **125**, 8798–8805 (2003).
8. A. Hinman, J. Du Bois, *J. Am. Chem. Soc.* **125**, 11510–11511 (2003).
9. T. Nishikawa, D. Urabe, M. Isobe, *Angew. Chem. Int. Ed.* **43**, 4782–4785 (2004).
10. D. Urabe, T. Nishikawa, M. Isobe, *Chem. Asian J.* **1**, 125–135 (2006).
11. K. Sato *et al*., *J. Org. Chem.* **70**, 7496–7504 (2005).
12. K. Sato *et al*., *J. Org. Chem.* **73**, 1234–1242 (2008).
13. S. Akai *et al*., *Bull. Chem. Soc. Jpn.* **83**, 279–287 (2010).
14. T. Maehara, K. Motoyama, T. Toma, S. Yokoshima, T. Fukuyama, *Angew. Chem. Int. Ed.* **56**, 1549–1552 (2017).
15. K. Murakami, T. Toma, T. Fukuyama, S. Yokoshima, *Angew. Chem. Int. Ed.* **59**, 6253–6257 (2020).
16. F. Cagide-Fagín, R. Alonso, *Eur. J. Org. Chem.* **2010**, 6741–6747 (2010).
17. H. Lago-Santomé, R. Meana-Pañeda, R. Alonso, *J. Org. Chem.* **79**, 4300–4305 (2014).
18. B. A. Mendelsohn, M. A. Ciufolini, *Org. Lett.* **11**, 4736–4739 (2009).
19. J. Chau, S. Xu, M. A. Ciufolini, *J. Org. Chem.* **78**, 11901–11910 (2013).
20. S. Xu, M. A. Ciufolini, *Org. Lett.* **17**, 2424–2427 (2015).
21. D. Baidilov *et al*., *Angew. Chem. Int. Ed.* **57**, 10994–10998 (2018).
22. K. Nishikawa *et al*., *Org. Lett.* **23**, 1703–1708 (2021).
23. J. G. Robins, J. S. Johnson, *Org. Lett.* **24**, 559–563 (2022).
24. R. J. Bergeron, J. S. McManis, *J. Org. Chem.* **52**, 1700–1703 (1987).
25. D. B. Konrad, B. Kicin, D. Trauner, *Synlett* **30**, 383–386 (2019).
26. J. Eames *et al*., *J. Chem. Soc., Perkin Trans. 1* **1999**, 1095–1104 (1999).
27. R. G. Soengas, A. M. S. Silva, *Eur. J. Org. Chem.* **2013**, 5022–5027 (2013).
28. T. Mukaiyama, T. Hoshino, *J. Am. Chem. Soc.* **82**, 5339–5342 (1960).
29. A. Hager, N. Vrielink, D. Hager, J. Lefranc, D. Trauner, *Nat. Prod. Rep.* **33**, 491–522 (2016).
30. Y. Basel, A. Hassner, *Synthesis* **1997**, 309–312 (1997).
31. K. N. Houk *et al*., *J. Am. Chem. Soc.* **106**, 3880–3882 (1984).
32. S. Diethelm, E. M. Carreira, *J. Am. Chem. Soc.* **137**, 6084–6096 (2015).
33. C. Cavedon *et al*., *Org. Lett.* **23**, 514–518 (2021).
34. B. M. Trost, Y. H. Rhee, *J. Am. Chem. Soc.* **121**, 11680–11683 (1999).
35. F. E. McDonald, K. S. Reddy, Y. Díaz, *J. Am. Chem. Soc.* **122**, 4304–4309 (2000).
36. M. J. Zacuto, D. Tomita, Z. Pirzada, F. Xu, *Org. Lett.* **12**, 684–687 (2010).
37. S. Beligny, S. Eibauer, S. Maechling, S. Blechert, *Angew. Chem. Int. Ed.* **45**, 1900–1903 (2006).
38. B. Plietker, *J. Org. Chem.* **68**, 7123–7125 (2003).
39. D. W. Knight, I. R. Morgan, A. J. Proctor, *Tetrahedron Lett.* **51**, 638–640 (2010).
40. K. Tsuda *et al*., *Chem. Pharm. Bull.* **12**, 1357–1374 (1964).
41. M. Yotsu-Yamashita, J.-H. Jang, Y. Cho, K. Konoki, *Forensic Toxicol.* **29**, 61–64 (2011).
42. K. Nakanishi, *Bioorg. Med. Chem.* **13**, 4987–5000 (2005).
43. I. J. Curcino Vieira, R. Braz-Filho, *Stud. Nat. Prod. Chem.* **33**, 433–492 (2006).
44. D. B. Konrad *et al*., Supplementary NMR-package for "A Concise Synthesis of Tetrodotoxin," Zenodo (2022). https://doi.org/10.5281/zenodo.6629561.

ACKNOWLEDGMENTS

We thank I. Žamarija, A. Novak, C. Wanzke, K. Schwärzer, E. Miller, R. Bechtel, N. Kurrle, and B. Kicin for experimental assistance and P. Mayer for x-ray analyses. **Funding:** We gratefully acknowledge financial support by the NSF (CHE-1900154). D.B.K. thanks the Friedrich-Ebert-Stiftung for a doctoral scholarship. K.P.R. and B.E.H. are supported by an NYU MacCracken Fellowship. H.A. was supported by the JSPS Overseas Challenge Program for Young Researchers. **Author contributions:** D.T. conceived and directed the project. B.S.M., D.B.K., K.P.R., and D.T. conceptualized and designed the synthetic strategy. B.S.M., D.B.K., K.P.R., H.A., and B.E.H. performed and analyzed the synthetic chemistry experiments. N.S. and K.N.H. performed computational studies. B.S.M., D.B.K., K.P.R., B.E.H., and D.T. prepared the manuscript. B.S.M., D.B.K., and D.T. acquired funding for the project. **Competing interests:** The authors declare that they have no competing interests. **Data and materials availability:** Crystallographic data for compounds **11** (CCDC 2117035) and **14** (CCDC 2117036) are available free of charge from the Cambridge Crystallographic Data Centre. Zipped free induction decay files for the NMR spectra of compounds **24**, **25**, **26**, **27**, **S4**, **S5**, and **TTX** have been deposited in Zenodo (*44*).

SUPPLEMENTARY MATERIALS

science.org/doi/10.1126/science.abn0571
Materials and Methods
NMR spectra
X-ray data
Calculations
Figs. S1 to S12
Tables S1 to S5
References (*45*–*66*)

Submitted 31 October 2021; accepted 15 June 2022
10.1126/science.abn0571

Science

A concise synthesis of tetrodotoxin

David B. KonradKlaus-Peter RühmannHiroyasu AndoBelinda E. HetzlerNina StrassnerKendall N. HoukBryan S. MatsuuraDirk Trauner

Science, 377 (6604), • DOI: 10.1126/science.abn0571

Tetrodotoxin by cycloaddition

Tetrodotoxin is a potent bacterial neurotoxin widely associated with pufferfish and thoroughly studied for its sodium channel–blocking properties. Its intricate structure of oxygen-rich interconnected rings has also long intrigued synthetic chemists. Konrad *et al*. report a comparatively concise route to the natural product from a glucose derivative. A dipolar cycloaddition enabled the formation of the cyclohexyl core at a later stage than prior approaches. Ruthenium catalysis was then key in assembling the surrounding oxygenated rings. —JSY

Science (ISSN) is published by the American Association for the Advancement of Science. 1200 New York Avenue NW, Washington, DC 20005. The title *Science* is a registered trademark of AAAS.